Selective Binding of Group IIIA and Lanthanide Metals by Hexahomotrioxacalix[3]arene Macrocycles

Charles E. Daitch,[1b] Philip D. Hampton,*[,1a] Eileen N. Duesler,[1a] and Todd M. Alam[1b]

Contribution from the Department of Chemistry, University of New Mexico, Albuquerque, New Mexico 87131, and Materials Aging and Reliability, Bulk Properties, Sandia National Laboratories, Albuquerque, New Mexico 87185

Received February 23, 1996[⊗]

Abstract: The hexahomotrioxacalix[3]arene macrocycles **1** are observed to bind trivalent metals (Sc^{3+}, Lu^{3+},Y^{3+}, La^{3+}) more strongly than alkali metal ions (Li^+, Na^+, K^+). Complexes of macrocycle **1a** with Lu(III) (**3**), Y(III) (**4**), and La(III) (**5**) have been structurally characterized to be μ-aryloxo-bridged dimers with the formula $[M(L)(DMSO)]_2$ (M = Lu, Y, La; L = trianion of macrocycle **1a**). Periodic trends in the structures and dynamic behavior of the complexes are discussed.

Introduction

The hexahomotrioxacalix[3]arene macrocycles **1**, abbreviated to "oxacalix[3]arenes" in this paper, are intriguing ligands for the separation of metal ions, since they are structurally related to the calixarenes and the crown ethers which have been shown to exhibit metal ion selectivity. In contrast with the extensive studies[2] of metal complexation by the calix[*n*]arene macrocycles, there have been only limited studies of the metal complexing ability of the oxacalix[3]arene macrocycles. We have previously reported a convenient synthesis of the oxacalix[3]arene macrocycles **1a**−**e** which allows for a range of *para* substituents.[3] Scandium(III) and titanium(IV) complexes of the oxacalix[3]-arenes have been synthesized and a $[Sc(L)(DMSO)]_2$ complex has been structurally characterized (L = the trianion of macrocycle **1a**).[4,5] Alkali-metal-binding studies of *O*-alkylated derivatives of macrocycle **1a** have been reported by Shinkai and co-workers.[6] An *O*-carboxymethyl derivative of macrocycle **1a** is observed to bind Pr(III), Eu(III), and Yb(III).[7]

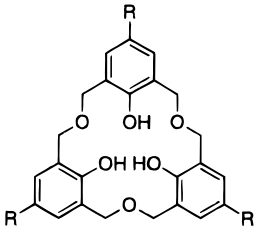

1a: R= *t*-Bu
1b: R= *i*-Pr
1c: R= Et
1d: R= Me
1e: R= Cl

In this paper, we report the synthesis and X-ray crystal structures of Lu(III) **3**, Y(III) **4**, and La(III) **5** complexes of the oxacalix[3]arene macrocycle **1a**. Periodic trends in the structures and dynamic NMR behavior of the complexes are discussed. Based on NMR titrations, the oxacalix[3]arene macrocycles **1** selectively bind trivalent metal ions over alkali metal ions.

Results

Synthesis and Characterization of the Lutetium, Yttrium and Lanthanum Complexes 3, 4, and 5. The reaction of *p-tert*-butyloxacalix[3]arene (**1a**) with $Y(OTf)_3$, $Lu(OTf)_3$, or $La(OTf)_3$ in a DMSO/acetonitrile mixture and an excess of triethylamine results in the crystallization of complexes **3**, **4**, and **5** which have the general formula $[M(L)(DMSO)]_2$ (M = Lu, Y, La). The isolated complexes **3**−**5** were characterized by ^{1}H NMR, elemental analyses, and X-ray crystallography.

The overall molecular configurations of complexes **3** and **5** are shown in Figures 1 and 2, respectively. Complex **4** is isostructural with complex **3** and the previously reported[4] Sc(III) complex **2**; an ORTEP diagram for complex **4** is provided in the supporting information. Table 1 provides crystallographic data and a summary of the data collection for the three complexes. Important structural features for the complexes **2**, **3**, **4**, and **5** are provided in Table 2. The numbering of the

⊗ Abstract published in *Advance ACS Abstracts,* August 1, 1996.

(1) (a) University of New Mexico. (b) Sandia National Laboratories.

(2) (a) Bott, S. G.; Coleman, A. W.; Atwood, J. L. *Chem. Commun.* **1986**, 610. (b) Atwood, J. L.; Orr, G. W.; Means, N. C.; Hamada, F.; Zhang, H.; Bott, S. G.; Robinson, K. D. *Inorg. Chem.* **1992**, *31*, 603. (c) Olmstead, M. M.; Sigel, G.; Hope, H.; Xu, X.; Power, P. P. *J. Am. Chem. Soc.* **1985**, *107*, 8087. (d) Xu, B.; Swager, T. M. *J. Am. Chem. Soc.* **1993**, *115*, 1159. (e) Harrowfield, J. M.; Ogden, M. I.; White, A. H. *Aust. J. Chem.* **1991**, *44*, 1237. (f) Engelhardt, L. M.; Furphy, B. M.; Harrowfield, J. M.; Kepert, D. L.; White, A. H.; Wilner, F. R. *Aust. J. Chem.* **1988**, *41*, 1465. (g) Furphy, B. M.; Harrowfield, J. M.; Kepert, D. L.; Skelton, B. W.; White, A. H.; Wilner, F. R. *Inorg. Chem.* **1987**, *26*, 4231. (h) Harrowfield, J. M.; Ogden, M. I.; White, A. H.; Wilner, F. R. *Aust. J. Chem.* **1989**, *42*, 949. (i) Furphy, B. M.; Harrowfield, J. M.; Ogden, M. I.; Skelton, B. W.; White, A. H.; Wilner, F. R. *J. Chem. Soc., Dalton Trans.* **1989**, 2217. (j) Bünzli, J.-C. G.; Froidevaux, P.; Harrowfield, J. M. *Inorg. Chem.* **1993**, *32*, 3306. (k) Asfari, Z.; Harrowfield, J. M.; Ogden, M. I.; Vicens, J.; White, A. H. *Angew. Chem., Int. Ed. Engl.* **1991**, *30*, 854. (l) Harrowfield, J. M.; Ogden, M. I.; White, A. H. *J. Chem. Soc., Dalton Trans.* **1991**, 979. (m) Assmus, R.; Böhmer, V.; Harrowfield, J. M.; Ogden, M. I.; Richmond, W. R.; Skelton, B. W.; White, A. H. *J. Chem. Soc., Dalton Trans.* **1993**, 2427. (n) Beer, P. D.; Drew, M. G.; Kan, M.; Leeson, P. B.; Ogden, M. I.; Williams, G. *Inorg. Chem.* **1996**, *35*, 2202.

(3) Hampton, P. D.; Bencze, Z.; Tong, W.; Daitch, C. E. *J. Org. Chem.* **1994**, *59*, 4838.

(4) Daitch, C. E.; Hampton, P. D.; Duesler, E. N. *Inorg. Chem.* **1995**, *34*, 5641.

(5) Hampton, P. D.; Daitch, C. E.; Alam, T. M.; Bencze, Z.; Rosay, M. *Inorg. Chem.* **1994**, *33*, 4750.

(6) (a) Araki, K.; Hashimoto, N.; Otsuka, H.; Shinkai, S. *J. Org. Chem.* **1993**, *58*, 5958. (b) Araki, K.; Inada, K.; Otsuka, H.; Shinkai, S. *Tetrahedron* **1993**, *49*, 9465. (c) Shinkai, S.; Takeshita, M.; Inokuchi, F. *Tetrahedron Lett.* **1995**, *36*, 3341.

(7) Arnaud-Neu, F. *Chem. Soc. Rev.* **1994**, 235.

S0002-7863(96)00598-7 CCC: $12.00

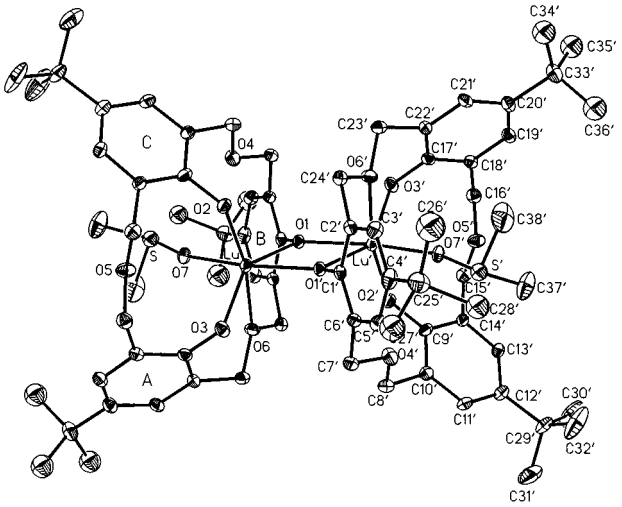

Figure 1. ORTEP diagram of $[Lu(L)(DMSO)]_2 \cdot (CH_3CN)_4(H_2O)_{0.67}$ (**3**) where L is the trianion of macrocycle **1a**. Ellipsoids are drawn at the 20% probability level. Primed and unprimed symbols denote atoms related by an inversion center.

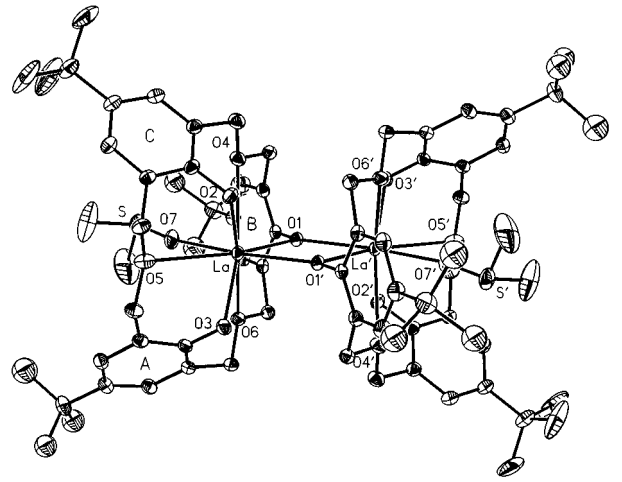

Figure 2. ORTEP diagram of $[La(L)(DMSO)]_2 \cdot (CH_3CN)_2(H_2O)$ (**5**) where L is the trianion of macrocycle **1a**. Ellipsoids are drawn at the 20% probability level. Primed and unprimed symbols denote atoms related by an inversion center.

macrocyclic atoms for complexes **2**, **4**, and **5** is the same as that for the Lu(III) complex **3** (Figure 1).

The determination of the structures of complexes **3**, **4**, and **5** was complicated by the high thermal motion and associated disorder of the *tert*-butyl groups, the coordinated DMSO molecule, and the molecules of solvation. The structures were well-defined with respect to the metal environment and core atoms of the ligand.

Complexes **3**, **4**, and **5** are centrosymmetric dimers that possess a $M_2(\mu\text{-}O)_2$ core (M = Lu, Y, La) where two macrocycle aryloxide oxygens (O1 and O1′) are the bridging oxygens (Figures 1 and 2). The lutetium (**3**) and yttrium (**4**) complexes are six-coordinate with distorted octahedral metal centers. Three aryloxide oxygens (O1, O2, O3) occupy meridonal coordination sites in the complexes with one coordinated macrocycle ether (O6) linkage completing the basal plane; a μ-aryloxo linkage (O1′) and a unidentate DMSO occupy the remaining metal coordination sites.

In contrast with complexes **3** and **4**, the metal centers in the dimeric lanthanum complex **5** are eight-coordinate with a distorted cubic geometry. Opposite corners of the cube are occupied by the bridging aryloxide linkage (O1′) and the coordinated DMSO (O7); the three aryloxide oxygens (O1, O2, O3) and the three macrocycle ether (O4, O5, O6) linkages occupy the remaining coordination sites. The distortion is evident in the average O−La−O bond angle between adjacent macrocycle oxygen atoms (average 66.9°), the macrocycle

Table 1. Crystallographic Data and Summary of Data Collection and Structure Refinement[a]

	3	**4**	**5**
formula	$C_{42}H_{57.7}LuN_2O_{7.3}S$	$C_{40}H_{56}YNO_8S$	$C_{40}H_{55}LaNO_{7.5}S$
fw	914.4	799.8	840.8
cryst system	triclinic	triclinic	triclinic
space group	$P\bar{1}$	$P\bar{1}$	$P\bar{1}$
a, Å	11.941(1)	11.962(1)	12.022(1)
b, Å	14.515(2)	14.470(2)	14.239(2)
c, Å	15.893(2)	15.924(2)	16.061(3)
α, deg	64.59(1)	64.87(8)	66.23(1)
β, deg	69.58(1)	69.93(7)	71.16(1)
γ, deg	85.03(1)	85.20(7)	86.46(1)
V, Å^3	2325	2337	2374
Z	2	2	2
ρ_{calcd}, g cm^{-3}	1.306	1.136	1.176
crystal dims, mm	0.18 × 0.23 × 0.34	0.25 × 0.43 × 0.46	0.51 × 0.69 × 0.92
μ, cm^{-1}	22.1	13.4	9.8
2θ limits, deg	52	50	50
octants	$\pm h \pm k \pm l$	$\pm h \pm k \pm l$	$\pm h \pm k \pm l$
transm.	0.862−0.925	0.853−0.967	0.803−0.987
N	8704 (R_{int} = 2.9%)	7393 (R_{int} = 3.5%)	7916 (R_{int} = 1.8%)
N_o	6272	3465	6956
$R(F_o)^b$	0.042	0.085	0.052
$R_w(F_o)^c$	0.038	0.079	0.055

[a] λ = 0.7107 Å for all measurements. [b] $R(F_o) = \sum(|F_o| - |F_c|)/\sum|F_o|$. [c] $R_w(F_o) = [\sum(w(F_o - F_c)^2)/\sum(wF_o^2)]^{1/2}$.

Table 2. Structural Parameters and Free Energies of Activation ($\Delta G^{\ddagger}$) for Complexes **2**−**5**

	2[a]	**3**	**4**	**5**
Ln−O1[b]	2.101(8)	2.249(4)	2.293(8)	2.425(3)
Ln−O2[b]	1.979(8)	2.109(5)	2.149(13)	2.314(4)
Ln−O3[b]	1.960(8)	2.092(6)	2.150(10)	2.290(5)
Ln−O1′[b]	2.150(8)	2.245(4)	2.300(8)	2.467(3)
Ln−O4[b]				3.133(5)
Ln−O5[b]				2.824(5)
Ln−O6[b]	2.535(8)	2.488(7)	2.565(14)	2.995(5)
Ln−O7[b]	2.055(8)	2.152(5)	2.168(9)	2.386(5)
Ln−Ln[b]	3.427(5)	3.653(1)	3.748(3)	4.098(1)
O1−Ln−O2[c]	108.0(3)	141.6(2)	112.5(4)	109.8(2)
O1−Ln−O3[c]	141.1(3)	109.5(2)	137.2(4)	114.7(2)
O2−Ln−O3[c]	108.0(3)	105.5(2)	105.7(4)	122.7(1)
Ln−O1−Ln′[c]	107.4(3)	108.7(2)	109.4(4)	113.8(2)
Ln−O1−C1[c]	118.6(7)	113.9(3)	111.6(7)	106.7(2)
Ln−O2−C9[c]	139.7(8)	133.7(6)	132.0(12)	117.3(4)
Ln−O3−C17[c]	126.8(8)	118.6(4)	116.9(9)	111.8(3)
ΦA[d]	58.3(3)	61.8(2)	62.0(2)	62.0(2)
ΦB[d]	42.5(3)	55.5(2)	55.5(2)	55.5(2)
ΦC[d]	34.9(3)	39.4(3)	40.4(2)	47.3(2)
d[e]	0.186	0.219	0.262	0.487
n[f]	1	1	1	3
coord no.	6	6	6	8
metal size[g]	0.89	1.00	1.04	1.30
$\Delta G^{\ddagger}$ (T_c)[h]	16.9 (330)	12.2 (250)	11.4 (235)	10.6 (220)

[a] Data taken from ref 4. [b] Values are in Å. [c] Values are in deg. [d] Angle between the mean planes of the phenyl rings **A**, **B**, and **C** and the plane defined by O1, O2, and O3. The letters **A**, **B**, and **C** correspond to the phenyl rings labeled in Figures 1 and 2. The atom labeling for complexes **2**, **4**, and **5** is the same as for complex **3**. [e] Displacement of metal out of the plane of the phenolic oxygens (O1, O2, O3) and into the macrocycle cup in Å. [f] Number of coordinated ether linkages (O4, O5, O6). [g] Metal size is based on crystal radii (in Å) for the six-coordinate [Sc(III), Lu(III), Y(III)] and eight-coordinate [La(III)] metal ions; data taken from ref 20. [h] The free energies of activation ($\Delta G^{\ddagger}$) at the coalescence temperature [T_c (K), in parentheses] were calculated as discussed in the text.

aryloxide oxygens (O1, O2, O3) and the μ-aryloxo linkage (O1′) (average 78.5°), and the macrocycle ether oxygens (O4, O5, O6) and the coordinated DMSO (O7) (average 70.9°). Except for the latter value, these angles deviate substantially from that expected for a perfect cube (70.4°).

The macrocycle ligand in complexes **3**−**5** adopts a "cup" conformation similar to the metal complexes of the calix[*n*]-arenes and bishomooxacalix[4]arenes, where the metal is the base of the cup.[2] In each of the complexes **2**−**5**, the metals lie out of the plane of the phenolic oxygens and within the macrocycle cup. Dihedral angles between the aryl rings and the plane containing the phenolic oxygens can be used to define the pitch of the cup, where a greater dihedral angle indicates a steeper cup. The out-of-plane displacements (*d*) and dihedral angles (Φ) for complexes **2**−**5** are listed in Table 2. The pitch is observed to increase as the metal size increases [Sc (*ca.* 45.2°) < Lu (*ca.* 52.2°) < Y (*ca.* 52.6°) < La (*ca.* 54.9°)], indicating a greater distortion of the macrocycle. The dihedral angles in complexes **2**−**5** are considerably larger than those for the uncomplexed oxacalix[3]arene macrocycles **1a**[8] (38.3°, 38.3°, 34.4°) and **1b**[9] (34.6°, 33.5°, 29.6°).

Consistent with periodic trends, the Ln−O2 and Ln−O3 bond lengths for complexes **2**−**5** increase as the ionic radius of the metal increases. In addition, the bridging Ln−O1 bond distances are longer than the Ln−O2 and Ln−O3 bond distances as expected for μ-aryloxo linkages. Complexes **3**−**5** have longer M−OAr bond lengths and smaller M−O−C bond angles compared to previously characterized lanthanide aryloxide complexes which possess bulky aryloxide ligands.[2n,10−17] This suggests that there is probably reduced π-bonding in complexes **2**−**5** compared to the literature compounds.

Metal Complexation by the Oxacalix[3]arenes. The effect of base strength on metal binding was examined by titrating a 1:1 mixture of $M(OTf)_3$ (M = Sc, Lu, Y, La) and macrocycle **1a** with organic bases in DMSO-d_6 and observing ^{1}H NMR spectral changes. The addition of a stoichiometric amount of imidazole (3 equiv, pK_a 6.2) to a mixture of **1a** and $Sc(OTf)_3$ resulted in the disappearance of the singlet[3] (4.64 ppm) for the methylene protons in **1a** and the appearance of a pair of doublets. With $Lu(OTf)_3$ and $Y(OTf)_3$, metal complex formation was incomplete with imidazole as a base but stoichiometric with 3 equiv of 1,4-diazabicyclo[2.2.2]octane (DABCO, pK_a 8.5). Binding of $La(OTf)_3$ to macrocycle **1a** was incomplete even in the presence of a large excess of triethylamine (pK_a 9.0).[18] The spectra of the metal complexes formed in each of these titrations were identical to that of the isolated complexes **2**−**5** in DMSO-d_6; no other metal−macrocycle complexes were observed during the titrations.

Dynamic NMR Studies. In toluene-d_8, complexes **2**−**5** exhibit dynamic behavior consistent with the isomerization of the μ-aryloxo-bridged dimers. The high temperature spectrum for all three complexes consists of doublets for the methylene protons and a singlet for the *tert*-butyl protons. At low temperatures, the complexes exhibit six doublets for the methylene protons and two *tert*-butyl singlets (2:1 integral ratio). Table 2 lists the coalescence temperature (T_c) and the free energy of activation ($\Delta G^{\ddagger}$) at the coalescence temperature for each of the complexes. The activation energies at coalescence were calculated using eq 1 for an unequally populated, two-site

$$k_{ex} = \frac{2(2\pi\Delta\upsilon)}{3X} \qquad (1)$$

exchange mechanism.[19] A line shape simulation was performed on the lanthanum(III) complex **5** to confirm the validity of eq 1; the activation energy (11.2 kcal/mol) at the coalescence temperature (220−225 K) is similar to the value obtained using eq 1 (10.6 kcal/mol, Table 2).[19] The activation enthalpy ($\Delta H^{\ddagger}$) and entropy ($\Delta S^{\ddagger}$) of complex **5** obtained from the simulation were determined to be 12.8 kcal/mol and 7.2 cal/(K·mol), respectively. Experimental details of the simulation are provided in the supporting information.

Discussion

Although the oxacalix[3]arene macrocycles could act as mono-, di-, or trianionic donors to a trivalent metal center, X-ray crystallographic studies and NMR titrations indicate the formation of metal complexes with only the macrocycle trianion. Complexes **2**−**5** are dimeric in the solid state and in non-coordinating solvents (toluene), whereas they dissociate to form monomeric $[M(L)(DMSO)_n]$ (n = 2−3) complexes in DMSO.

Macrocycle **1a** exhibits a remarkable ability to accommodate the binding of trivalent metals with a range of crystal radii[20] (Table 2: six-coordinate Sc(III) 0.89 Å, eight-coordinate La-(III) 1.30 Å). Larger metals result in increased macrocycle cupping and a slightly greater displacement of the metal out of the plane of the phenolic oxygens into the macrocycle cup (Φ and *d*, Table 2). In contrast, the calix[*n*]arenes tend to accommodate different metal sizes through changes in the mode of metal binding to the macrocycle.[2] The conformational flexibility of the oxacalix[3]arenes is probably responsible for this difference. Gutsche and co-workers have reported that the oxacalix[3]arene macrocycles **1** are more flexible than the calix-[*n*]arenes based on dynamic ^{1}H NMR studies.[21]

The coordination of metals to the oxacalix[3]arenes exhibits both unusual coordination numbers and geometries. The

(8) Suzuki, K.; Minami, H.; Yamagata, Y.; Fujii, S.; Tomita, K.; Asfari, Z.; Vicens, J. *Acta Crystallogr.* **1992**, *C48*, 350.

(9) Z. Bencze, Ph.D. Thesis, University of New Mexico, 1995.

(10) The average Ln−OAr bond lengths and Ln−O−C bond angles in complexes **3**−**5** are the following: Lu−O *ca.* 2.10 Å, ∠Lu−O−C *ca.* 122°, Y−O *ca.* 2.15 Å, ∠Y−O−C *ca.* 120°, La−O *ca.* 2.30 Å, and ∠La−O−C *ca.* 112°. Similar Lu−O (2.06 Å) and somewhat shorter La−O (2.23 Å) bond lengths are observed for [M(L′)(picrate)(H_2O)] complexes [M = Lu, La; L′ = dianion of 1,3-bis(diethylamide) derivative of *p-tert*-butylcalix-[4]arene].[1n]

(11) Lu(O-2,6-*i*-$Pr_2C_6H_3)_3(THF)_2$ (Lu−O *ca.* 2.045 Å, ∠Lu−O−C 174°, 174°, and 153°): Barnhart, D. M.; Clark, D. L.; Gordon, J. C.; Huffman, J. C.; Vincent, R. L.; Watkin, J. G.; Zwick, B. D. *Inorg. Chem.* **1994**, *33*, 3487.

(12) Y(O-2,6-*t*-$Bu_2C_6H_3)_3$ (Y−O *ca.* 2.00 Å, ∠Y−O−C *ca.* 173°): Hitchcock, P. B.; Lappert, M. F.; Smith, R. G. *Inorg. Chim. Acta* **1987**, *139*, 183.

(13) Y(C_5Me_5)(O-2,6-*t*-$Bu_2C_6H_3)_3$ (Y−O *ca.* 2.08 Å, ∠Y−O−C 168° and 129°): Schaverien, C. J.; Frijns, J. H. G.; Heeres, H. J.; van den Hende, J. R.; Teuben, J. H.; Spek, A. L. *Chem. Commun.* **1991**, 642.

(14) La(O-2,6-$Ph_2C_6H_3)_3(THF)_2$ (La−O *ca.* 2.24 Å, ∠La−O−C *ca.* 162°): Deacon, G. B.; Gatehouse, B. M.; Shen, Q.; Ward, G. N. *Polyhedron* **1993**, *12*, 1289.

(15) La(O-2,6-*i*-$Pr_2C_6H_3)_3(THF)_2$ (La−O *ca.* 2.21 Å, ∠La−O−C 173°, 173°, and 152°): Butcher, R. J.; Clark, D. L.; Grumbine, S. K.; Vincent-Hollis, R. L.; Scott, B. L.; Watkin, J. G. *Inorg. Chem.* **1995**, *34*, 5468.

(16) K[La(O-2,6-*i*-$Pr_2C_6H_3)_4$] (La−O *ca.* 2.24 Å, ∠La−O−C *ca.* 161°): Clark, D. L.; Gordon, J. C.; Huffman, J. C.; Vincent-Hollis, R. L.; Watkin, J. G.; Zwick, B. D. *Inorg. Chem.* **1994**, *33*, 5903.

(17) (THF)La(O-2,6-*i*-$Pr_2C_6H_3)_2$(μ-O-2,6-*i*-$Pr_2C_6H_3)_2Na(THF)_2$ (terminal aryloxides only, La−O *ca.* 2.23 Å, ∠La−O−C 171°): Clark, D. L.; Hollis, R. L.; Scott, B. L.; Watkin, J. G. *Inorg. Chem.* **1996**, *35*, 667.

(18) (a) pK_a's of the conjugate acids of imidazole (6.2) and DABCO (8.5) in DMSO: Bordwell, F. G.; Liu, W., personnel communication, 1995. (b) pK_a of the conjugate acid of triethylamine (9.0) in DMSO: Kolthoff, I. M.; Chantooni, M. K., Jr.; Bhowmik, S. *J. Am. Chem. Soc.* **1968**, *90*, 23.

(19) Sandström, J. *Dynamic NMR Spectroscopy*; Academic Press: London, 1982; pp 81−84. Table 6.1 in this reference indicates that X = 2.0823 when the difference in population (Δp) of the sites is 0.333. The additional factor of two-thirds in eq 2 results from treating the three-site macrocycle exchange with two equivalent sites (supporting information) as a two-site exchange with unequal exchange probabilities.

(20) Shannon, R. D. *Acta Crystallogr.* **1976**, *A32*, 751.

(21) Gutsche, C. D.; Bauer, L. J. *J. Am. Chem. Soc.* **1985**, *107*, 6052.

octahedral structure in the Lu(III) **3** and Y(III) **4** complexes is in contrast with the tendency for higher coordination numbers (seven- or eight-coordinate) for metals in the lanthanide series.[22] The cubic geometry of the La(III) centers in complex **5** is relatively uncommon for eight-coordinate complexes.[23,24] A theoretical analysis by Hoffmann and co-workers determined that the cubic geometry is less stable than the more common dodecahedron and square antiprism geometries as a result of steric and electronic effects.[23a]

Estimates of the metal-binding affinity of the oxacalix[3]arene macrocycles toward monovalent and trivalent metals can be obtained by comparing the strength of the base that is needed for stoichiometric metal binding to be observed. In a previous paper, we reported that macrocycle **1a** exhibited no affinity toward monovalent metals (Li, Na, K) even in the presence of a large excess of triethylamine.[3] In contrast, each of the trivalent metals examined in this study were observed to bind in the presence of an organic base; the metal binding affinity increases as the charge-to-radius ratio increases for the metal ion [Sc^{3+} > Lu^{3+}, Y^{3+} > La^{3+} > Li^{+}, Na^{+}, K^{+}].[25] Studies are in progress to determine binding constants for trivalent metals with macrocycles **1a**−**e**.

Each of the complexes **2**−**5** exhibit dynamic behavior on the ^{1}H NMR time scale in toluene-d_8. The spectral changes are consistent with cleavage of a μ-aryloxo linkage followed by rotation about the remaining μ-aryloxo linkage.[4] The positive $\Delta S^{\ddagger}$ value obtained for complex **5** is consistent with this proposed mechanism. The trend in the $\Delta G^{\ddagger}$ values for complexes **2**−**5** indicates that the free energy of activation decreases as the metal size increases. This is consistent with the expected trend of decreasing strength of a μ-aryloxo linkage with increasing metal size.

Conclusion

Group IIIA and lanthanide complexes of the oxacalix[3]arene macrocycles **1** can be readily synthesized by the reaction of macrocycle **1a** with a metal triflate in the presence of triethylamine. The scandium(III), lutetium(III), yttrium(III), and lanthanum(III) complexes are dimers possessing similar structures where the oxacalix[3]arene macrocycle **1a** acts as a trianionic donor to the metal center. The number of coordinated macrocycle ether oxygens and the degree of cupping of the macrocycle are observed to increase, and the μ-aryloxo bond strength is observed to decrease as the metal size increases. In addition to allowing for the coordination of a wide range of metal sizes, the oxacalix[3]arene macrocycles enforce low coordination numbers for Lu(III) and Y(III), and an unusual cubic coordination geometry for La(III).

Experimental Section

General Procedures. Solvents and triethylamine were dried using either calcium hydride or sodium benzophenone ketyl and degassed. Dimethyl sulfoxide was dried over 4 Å molecular sieves. *p-tert*-Butyloxacalix[3]arene[3] and lanthanide trifluoromethanesulfonates[26] [Ln(OTf)$_3$, Ln = Sc, Y, La] were prepared following literature procedures. Lutetium trifluoromethanesulfonate was purchased (Aldrich) and used without purification. The synthesis of complex **2** has previously been reported.[4] The lanthanide complexes **3**, **4**, and **5** were prepared and handled under inert atmosphere using either Schlenk or drybox techniques. NMR spectra were recorded on a Bruker AC-250 at resonant frequencies of 250 and 62.9 MHz for ^{1}H and ^{13}C, respectively. Chemical shifts were referenced to either tetramethylsilane or protio solvent impurity. Elemental analyses were performed by Galbraith Laboratories and Dr. Ruby Ju.

Synthesis of [Lu(L)(DMSO)]$_2$·(CH$_3$CN)$_4$(H$_2$O)$_{0.67}$ (3). In an inert atmosphere glovebox a solution of 47 mg of Lu(OTf)$_3$ (0.076 mmol) in 1 mL of DMSO was added to a solution of 40 mg of *p-tert*-butyloxacalix[3]arene (0.069 mmol) and 30 mg of triethylamine (0.29 mmol) in 4 mL of acetone. The sample was heated to reflux and stirred for 2 min. Cooling over 24 h afforded the product **3** as yellow, prismatic crystals in 74% yield. ^{1}H NMR (toluene-d_8, 298 K): δ 7.11 (s, 6H, 3,5-aryl protons), 5.74 (d, J = 7.5 Hz, 6H, methylene protons), 4.08 (d, J = 7.5 Hz, 6H, methylene protons), 1.23 (s, 27H, *tert*-butyl protons), 0.52 (s, 6H, DMSO methyl protons). Anal. Calcd for $C_{42}H_{57.67}LuN_2O_{7.33}S$: C, 55.14; H, 6.35. Found: C, 55.52; H, 6.35.

Synthesis of [Y(L)(DMSO)]$_2$·(CH$_3$CN)$_2$(H$_2$O)$_2$ (4). The same procedure was followed as for complex **3**. Complex **4** was obtained as pale yellow, block crystals in 83% yield. ^{1}H NMR (toluene-d_8, 298 K): δ 7.12 (s, 6H, 3,5-aryl protons), 5.78 (d, J = 7.5 Hz, 6H, methylene protons), 4.05 (d, J = 7.5 Hz, 6H, methylene protons), 1.24 (s, 27H, *tert*-butyl protons). Anal. Calcd for $C_{40}H_{56}NO_8SY$: C, 60.07; H, 7.06. Found: C, 59.84; H, 6.82.

Synthesis of [La(L)(DMSO)]$_2$·(CH$_3$CN)$_2$(H$_2$O) (5). The procedure was the same as for complex **3** except the triethylamine was increased to 726 mg (7.2 mmol). Complex **5** was obtained as pale yellow, block crystals in 48% yield. ^{1}H NMR (toluene-d_8, 298 K): δ 7.09 (s, 6H, 3,5-aryl protons), 5.79 (d, J = 7.5 Hz, 6H, methylene protons), 3.97 (d, J = 7.5 Hz, 6H, methylene protons), 1.22 (s, 27H, *tert*-butyl protons). Anal. Calcd for $C_{40}H_{55}LaNO_{7.5}S$: C, 57.14; H, 6.59. Found: C, 57.48; H, 6.74.

X-ray Crystallographic Studies. For X-ray diffraction studies, crystals were sealed in capillaries wet with the supernatant solution. A total of N independent reflections were measured on a Siemens R3m/V diffractometer (293 K) using graphite monochromated Mo Kα radiation, λ = 0.71073 Å, with ω scan mode, within the specified $2\theta_{max}$ limit. After absorption correction (semiempirical), the structures were solved by Patterson map interpretation using SHELXTL PC and refined by the full-matrix least-squares method;[27] scattering factors were taken from the literature.[28] Anisotropic thermal parameters were refined for all non-hydrogen atoms except those in which the final difference Fourier map displayed signs of disorder (**3**: DMSO sulfur, acetonitrile, and water of solvation; **4**: DMSO sulfur, *tert*-butyl methyls on C25 and C33, acetonitrile, and water of solvation; **5**: DMSO sulfur, *tert*-butyl methyls on C29 and C33, and waters of solvation). No corrections for extinction were made. Hydrogen atoms were calculated and allowed to ride on the carbon atom to which they were bonded with fixed U values except for disordered atoms. The final agreement factors R and R_w for N_o observed reflections having $F > 2.0\sigma(F)$, the function minimized being $\sum w(\Delta F^2)$ [statistical weights derived from $w^{-1} = \sigma^2(F) + 0.0030F^2$], are quoted. Crystallographic data and basic details of data collection for **3**, **4**, and **5** are presented in Tables 1 and 2.

Estimation of Free Energies of Activation. At low temperatures, complexes **2**−**5** exhibit two *tert*-butyl signals that coalesce to a singlet at high temperatures. The frequency separation ($\Delta\nu$) between the two *tert*-butyl signals at low temperature can be converted to an exchange rate constant (k_{ex}) using eq 1, and a $\Delta G^{\ddagger}$ can be calculated at the coalescence temperature (T_c) for each of the complexes.[19] The frequency separations ($\Delta\nu$) and rate constants (k_{ex}) for the complexes were the following: **2** 22.5 Hz, 45.3 s^{-1}; **3** 60.4 Hz, 122 s^{-1}; **4** 67.5 Hz, 136 s^{-1}; **5** 70.2 Hz, 141 s^{-1}. The $\Delta\nu$ were determined at low

(22) Cotton, F. A.; Wilkinson, G. *Advanced Inorganic Chemistry*, 5th ed.; John Wiley and Sons: New York, 1980; pp 985−987.

(23) (a) Burdett, J. K.; Hoffmann, R.; Fay, R. C. *Inorg. Chem.* **1978**, *17*, 2553 and references therein. (b) Muetterties, E. L.; Wright, C. M. *Q. Rev., Chem. Soc.* **1967**, *21*, 109. (c) Lippard, S. J. *Prog. Inorg. Chem.* **1967**, *8*, 109. (d) Sinha, S. P. *Struct. Bonding* **1976**, *25*, 69.

(24) The eight coordinate [La(L″)$_4$](ClO$_4$)$_3$ complex (L″ = 2,3′-bipyridine dioxide) is reported to have a cubic structure: Al-Karaghouli, A. R.; Day, R. O.; Wood, J. S. *Inorg. Chem.* **1978**, *17*, 3702.

(25) The charge-to-radius ratios (Å^{-1}) for monovalent and trivalent metals are the following, K^+ 0.66, Na^+ 0.86, Li^+ 1.1, La^{3+} 2.3, Y^{3+} 2.9, Lu^{3+} 3.0, Sc^{3+} 3.4. These ratios are based on metal crystal radii from ref 20 for the six- (Li, Na, K, Sc, Lu, Y) and eight- (La) coordinate metals.

(26) Kobayashi, S.; Hachiya, I.; Araki, M.; Ishitani, H. *Tetrahedron Lett.* **1993**, *34*, 3755.

(27) SHELXTL PC, Siemens Analytical X-Ray Instruments, Inc., 1990.

(28) *International Tables for X-ray Crystallography*; Kynoch: Birmingham, England, 1974; Vol. IV, pp 99−100, 149.

temperatures (slow exchange region). Correction for the observed temperature dependence of $\Delta\nu$ (supporting information, eqs 1 and 2) resulted in a nearly identical $\Delta G^{\ddagger}$ for complex **5**. Table 2 lists the coalescence temperatures and the $\Delta G^{\ddagger}$ for each of the complexes.

Acknowledgment is made to the donors of the Petroleum Research Fund, administered by the American Chemical Society, and to Sandia National Laboratories for partial support of this research. We would like to thank Dr. Zsolt Bencze for providing samples of oxacalix[3]arene (**1a**). The NSF Chemical Instrumentation Program is acknowledged for providing a low field NMR spectrometer. This work was partially supported (T.M.A.) by the United States Department of Energy under contract DE-AC04-94AL85000. We would like to thank Prof. Frederick G. Bordwell and Dr. Wei-Zhong Liu for providing us with pK_a values.

Supporting Information Available: Tables of atomic coordinates, bond distances, bond angles, thermal parameters, and hydrogen atom positions for complexes **3**, **4**, and **5**, complete experimental details and results for the simulation of complex **5**, and an ORTEP diagram of complex **4** (42 pages). See any current masthead page for ordering and Internet access instructions.

JA9605984